LLNL-CONF-676780

Transparent Ceramic Scintillators for Gamma Spectroscopy and MeV Imaging

N. J. Cherepy

August 31, 2015

SPIE Optics and Photonics
San Diego, CA, United States
August 10, 2015 through August 14, 2015

Disclaimer

Transparent Ceramic Scintillators for Gamma Spectroscopy and MeV Imaging

N.J. Cherepy[1], Z.M. Seeley[1], S.A. Payne[1], E.L. Swanberg[1], P.R. Beck[1], D.J. Schneberk[1], G. Stone[1], R. Perry[1], B.M. Wihl[1], S.E. Fisher[1], S.L. Hunter[1], P.A. Thelin[1], R.R. Thompson[1], T. Stefanik[2], J. Kindem[3]

[1]Lawrence Livermore National Laboratory, Livermore, CA 94550 USA
[2]Nanocerox, Inc., Ann Arbor, MI 48108 USA
[3]Cokiya, Inc, San Diego, CA USA

ABSTRACT

We report on the development of two new mechanically rugged, high light yield transparent ceramic scintillators: (1) Ce-doped Gd-Garnet for gamma spectroscopy, and (2) Eu-doped Gd-Lu-Bixbyite for radiography. GYGAG(Ce) garnet transparent ceramics offer ρ = 5.8g/cm^3, Z_{eff} = 48, principal decay of <100 ns, and light yield of 50,000 Ph/MeV. Gd-Garnet ceramic scintillators offer the best energy resolution of any oxide scintillator, as good as R(662 keV) = 3% (Si-PD readout) for small sizes and typically R(662 keV) < 5% for cubic inch sizes. For radiography, the transparent ceramic scintillator, $(Gd,Lu,Eu)_2O_3$, or "GLO," offers excellent x-ray stopping, with ρ = 9.1 g/cm^3 and Z_{eff} = 68. Several 10" diameter by 0.1" thickness GLO scintillators have been fabricated. GLO outperforms scintillator glass for high energy radiography, due to higher light yield (55,000 Ph/MeV) and better stopping, while providing spatial resolution of >8 lp/mm.

Keywords: scintillators, gamma ray detection, transparent ceramics, radiography, X-ray imaging, garnets, bixbyites

1. INTRODUCTION

Transparent ceramics are an emerging class of optical materials, with applications including transparent armor, "unbreakable" windows, missile domes, lenses, laser gain media, and scintillators [1-6]. Transparent ceramics are polycrystalline, monolithic, fully-dense optics that offer advantages in lower processing temperatures, ease of fabrication of complex shapes and high aspect ratio optics (such as plates and fibers), and high, uniform doping, needed for high performance scintillators.

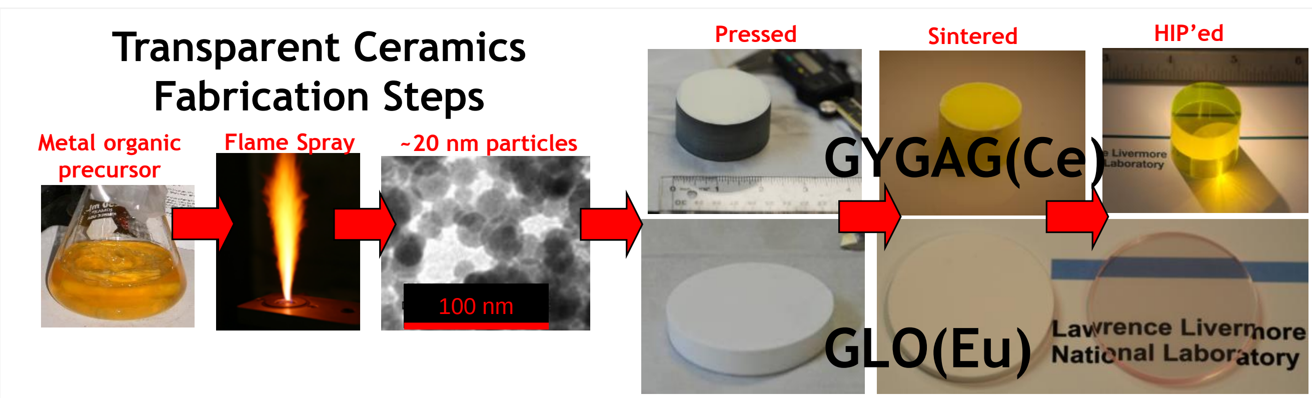

Figure 1. Flame spray pyrolysis nanopowders are synthesized from metal organic precursors, then pressed into a green body, sintered, hot-isostatic pressed and then polished to produce fully dense polycrystalline transparent ceramic optics.

Lawrence Livermore National Laboratory has developed a methodology for transparent ceramics fabrication that minimizes powder synthesis and milling steps by employing Flame Spray Pyrolysis (FSP) nanoparticles. Nanopowders are pressed into green bodies, sintered, then hot isostatic pressed and polished. Figure 1 describes the process steps used to fabricate transparent ceramics. We have used this route to fabricate two classes of scintillators – garnets and bixbyites.

Our work on the development of cerium-doped gadolinium garnets, including gadolinium yttrium gallium aluminum garnet, or GYGAG(Ce) is described in references [7-14]. Ceramics formed from line compounds like YAG must be synthesized with rigorous control over stoichiometry in order to avoid formation of secondary phases. In contrast, the mixed cation garnets, such as GYGAG offer a broad compositional range within which transparency may be achieved, since the intersubstutional ions (Y, Ga, Al) may substitute on more than one of the three garnet cation sites. The phase stability of GYGAG is robust, producing ceramics with high transparency, even when slightly off-stoichiometry, improving yield in fabrication and allowing flexibility in process parameters.

Bixbyite ceramics include Y_2O_3 and Lu_2O_3 and their variants. For high light yield, high doping with Eu into the bixbyite structure is required. However, Eu has limited solubility in Lu_2O_3, and above the 1% doping level, Eu-rich secondary phases form at the grain boundaries of Lu_2O_3. The secondary phases results due to limited solubility of Eu in Lu_2O_3 because of the mismatch of the ionic radii of Eu (95 pm) with Lu (86 pm). This can be mitigated by the addition of Gd (ionic radius of 94 pm), which we found to result in high transparency ceramics, without secondary phases [15]. Table 1 addresses sources of scatter and mitigation strategies for achieving transparency in ceramic optics.

Table 1. To achieve transparency in ceramics, all sources of optical scatter must be minimized.

Causes of optical scatter	**Mitigation**
Grain boundaries – light may be refracted as it crosses grain boundaries in birefringent crystalline structures	Select cubic/isotropic crystals structures, since they have isotropic refractive indices (no birefringence) so that no refraction can occur at grain boundaries.
Residual porosity	Optimize processing conditions to reduce pore sizes and minimize the presence of pores.
Secondary phases	Use high purity feedstock with controlled stoichiometry. Select cubic structures with broad phase stability under the temperature and pressure conditions used for consolidation. Intersubstitutional ions broaden the phase stability over a range of chemical compositions.

Most scintillator-based handheld gamma spectrometers today employ hygroscopic, fragile crystals, such as NaI(Tl) or $LaBr_3$(Ce). For field deployments, rugged instruments are needed that do not degrade or break in high humidity, fluctuating temperatures, or with mechanical shocks. The GYGAG(Ce) ceramic scintillator is unreactive with water and air, while additionally offering excellent fracture toughness. The GYGAG(Ce) scintillator also provides: (1) high, fast light yield of >40,000 Ph/MeV and principal decay of ~100 ns, (2) photopeak efficiency superior to NaI(Tl), (3) excellent light yield proportionality, (4) ease of uniform fabrication via ceramics processing, and (5) no intrinsic radioactivity.

Table 2. Gamma spectroscopy scintillators. GYGAG(Ce) compares favorably to the commercially available options.

Scintillator	**Density (g/cm^3)**	**Z_{eff}**	**Principal Decay (ns)**	**LY (Ph/keV)**	**Energy Resolution (% at 662 keV, typical)**
GYGAG, $Gd_{1.5}Y_{1.5}Ga_2Al_3O_{12}$(Ce)	5.80	48	100	50	4.6% (PMT), 3-3.5% (Si-PD)
YAG(Ce)	4.55	32	100	30	7%
CsI(Tl)	4.50	54	1500	65	6%
NaI(Tl)	3.67	51	230	40	6%
$LaBr_3$(Ce)	5.30	47	20	65	2.5-3%
SrI_2(Eu)	4.59	50	1200	100	2.5-3%

Imagers using high-energy Bremsstrahlung typically employ amorphous silicon flat panel imagers with optically scattering phosphor coatings, such as gadolinium oxysulfide. Though optically somewhat more complex, lens-coupled computed tomography (CT) systems with thin sheet free-standing transparent scintillators can achieve better spatial resolution [16]. The optics of these two types of scintillator screens are described in Figure 2.

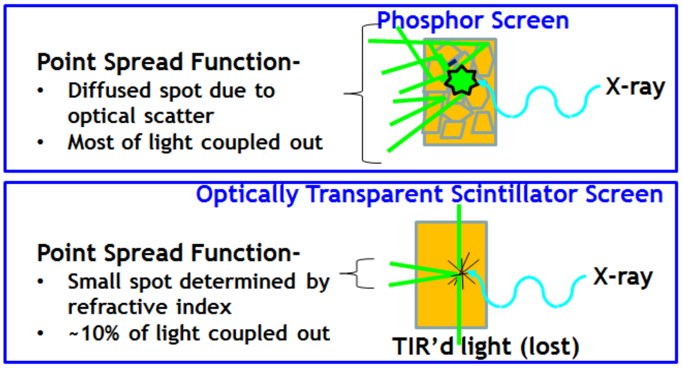

Figure 2. (top) Imaging with a phosphor screen results in blurring due to the optical scatter in the vicinity of where the scintillation light is produced. However, most of the light is coupled out of the scintillator screen. **(bottom)** Imaging with a transparent scintillator suffers from a lower effective light output, as most of the light is totally internally reflected, and only a small cone emerges from the front face of the scintillator. The advantage of this configuration is a much smaller spot size, as no optical scatter occurs.

For radiographic imaging fidelity and throughput, scintillators offering high stopping power, light yield, and radiation hardness are required. In comparison to single crystal CsI(Tl), $CdWO_4$ and LYSO(Ce), larger, optically contiguous plates can be obtained by ceramics processing. Another alternative, IQI glass, can be obtained in thin sheets, but its stopping power and light yield are low, as shown in Table 3. With a melting point of 2,490°C, melt growth of Lu_2O_3 and related crystals is not feasible. While Lu_2O_3(Eu) has long been recognized as an excellent candidate phosphor or ceramic for radiography [17-19], it has never previously been fabricated in large-size plates or with acceptably low optical scatter losses for implementation. We found transparent ceramic $Gd_{0.3}Lu_{1.6}Eu_{0.1}O_3$, or "GLO" offers excellent transparency, along with the high density and light yield needed to improve imaging performance and throughput.

Table 3. Comparison of scintillators for high energy X-ray imaging. The Figure-of-Merit is defined as α ×LY, normalized.

Scintillator	**ρ (g/cm^3)**	**α (cm^{-1}) @ 3 MeV**	**Light yield (Ph/MeV)**	**FOM**
GLO(Eu), $Gd_{0.3}Lu_{1.6}Eu_{0.1}O_3$	9.1	0.36	55,000	7.1
CsI(Tl)	4.5	0.17	65,000	3.9
$CdWO_4$	7.9	0.30	28,000	3.1
LYSO, $Lu_{1.9}Y_{0.1}SiO_5$(Ce)	7.1	0.28	27,000	2.7
IQI glass	3.8	0.14	20,000	1.0

2. EQUIPMENT AND METHODS

Transparent ceramic garnet scintillators were fabricated at LLNL using stoichiometric mixed metal oxide particles synthesized via flame spray pyrolysis (FSP), a nanoparticle production method developed by Pratsinis and co-workers [20] and by Laine and co-workers [21]. The transparent ceramics fabrication steps are detailed in Figure 1.

Gamma spectra with PMT readout and with silicon photodiode readout were acquired as described in [13, 22]. Spectra were analyzed off-line by non-linear least squares fitting to a Gaussian in order to estimate the energy resolution. Light yields were measured by comparison to a standard YAG(Ce) ceramic from Baikowski.

Attenuation radiographs and computed tomography images acquired using a Varian Linatron MI9 9 MeV Bremsstrahlung source, lead collimators, a rotating platform for the object, scintillator plate, turning mirror, imaging lens (200 mm Nikon Micro-Nikkor) and a CCD camera (Spectral Instruments). Images were analyzed using IMGREC software [23].

3. RESULTS AND DISCUSSION

3.1 Gamma Ray Spectroscopy with GYGAG(Ce)

Gamma spectroscopy with GYGAG(Ce) offers excellent proportionality, as previously reported [24], for good energy resolution from the few keV to the high MeV energy range. Figure 3 shows pulse height spectra with ^{137}Cs acquired with 2 in^3 size GYGAG(Ce), using PMT readout, obtaining R(662 keV) = 4.6%. With silicon photodiode readout, a single pixel of 0.05 cm^3 size can provide R(662 keV) = 3.0%. When co-adding the full array of 1024 pixels, energy resolution is slightly degraded. Current performance for the 1024 pixel array populated with a total GYGAG(Ce) volume of 3.4 in^3 offers R(662 keV) < 4% for photopeak events only, and R(662 keV) < 5% for photopeak plus Compton summed events [25]. The detector as a whole, shown in Figure 4, is designed for ruggedness, employing a Digirad solid-state silicon photodiode array readout, and garnet ceramics cuboids matched to the small photodiodes required for low dark current.

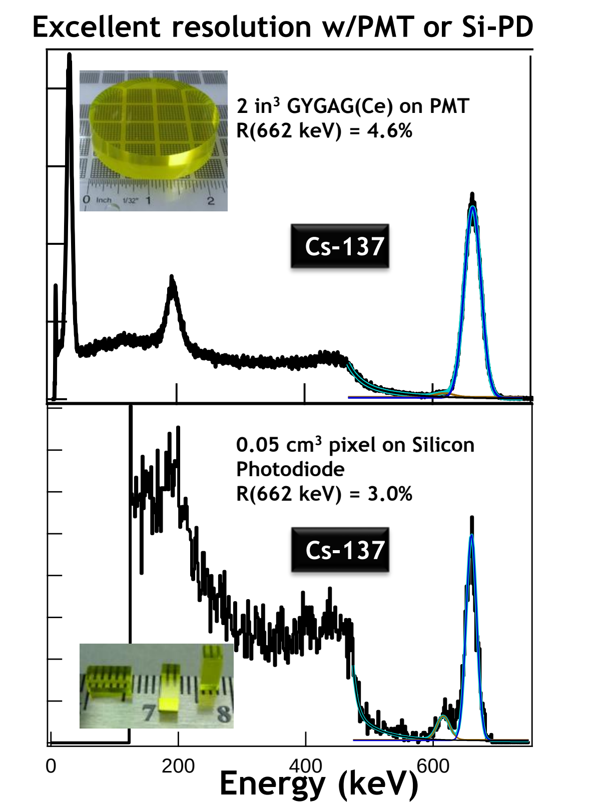

Figure 3. Gamma spectra acquired with GYGAG(Ce) transparent ceramics fabricated at LLNL. **(top)** A large ceramic scintillator with PMT readout provides 4.6% resolution at 662 keV, while **(bottom)** a single 3 mm x 3 mm x 6 mm pixel achieves 3.0% resolution with Silicon photodiode readout.

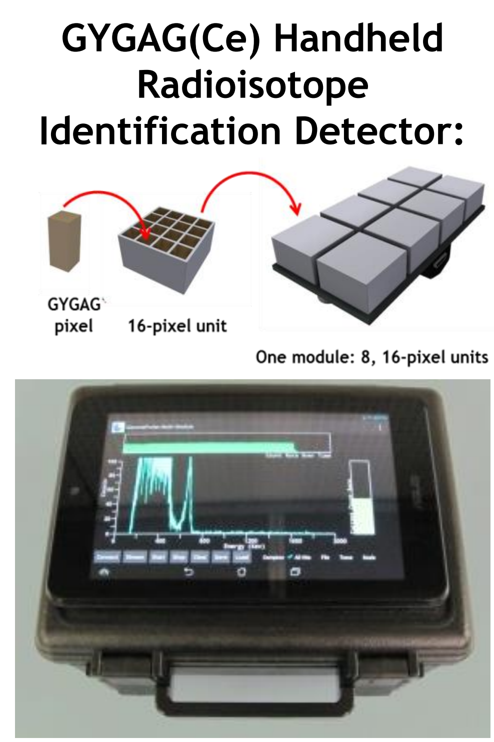

Figure 4. Pixelated GYGAG(Ce) gamma spectrometer.

- 1024, 3x3x6 mm pixels (55.3 cm^3/3.4 in^3 GYGAG)
- Eight modules, each has own ASIC and microcontroller, thermoelectric cooler
- Modules communicate to embedded computer
- Wireless readout via Android tablet
- Temperature stabilized low-noise Si photodiodes
- Co-add pixel spectra → Device-level spectra
- Compton summing to increase efficiency and tracking to provide directional detection

3.2 MeV Radiographic Imaging with GLO(Eu)

A typical arrangement for lens-coupled imaging radiography is described in Figure 5. The image is projected onto a CCD camera and recorded electronically, allowing efficient computed tomographic characterization.

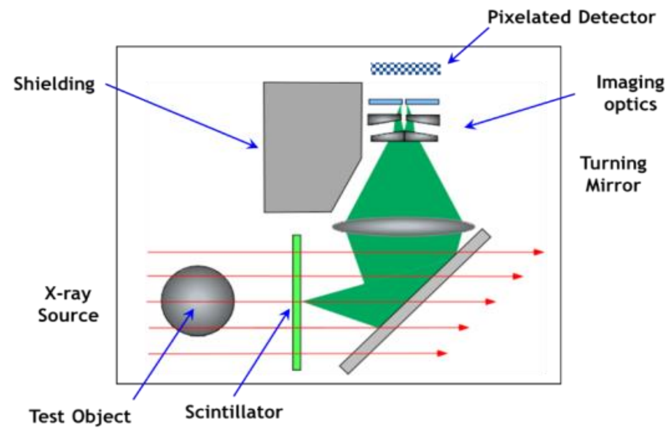

Figure 5. Experimental arrangement for lens-coupled radiography. Collimated X-rays interact with the object, and the image is formed in a free-standing transparent scintillator sheet. The image is reflected by a turning mirror, into imaging optics and then recorded by a high performance CCD camera.

For large field-of-view imagery, a large monolithic transparent scintillator is required. Figure 6 shows one of the 10" GLO samples currently being tested to establish performance for 9 MeV imaging.

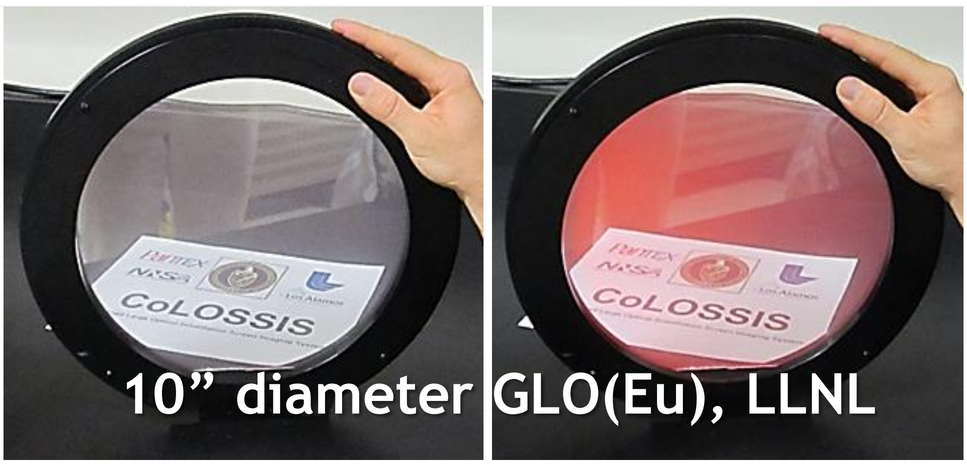

Figure 6. A 10" diameter by 0.1" thick transparent ceramic GLO(Eu) scintillator fabricated by LLNL. **(left)** GLO scintillator under room lights. The paper laying on the benchtop behind the scintillator is clearly readable at a standoff of >10", demonstrating the excellent transparency of the scintillator. **(right)** Same scintillator, under UV excitation, produces orange-red emission from Eu^{3+}, the same emission produced during scintillation.

Attenuation radiographs as well as computer tomography studies were performed, using the two scintillators, GLO(Eu) ceramic and IQI(Tb) glass. Attenuation radiographs were acquired with a ^{238}U penetrameter and modulation transfer function (MTF) fits were performed on edge features in order to obtain the spatial resolution. Additional radiographs were acquired with a single crystal nickel turbine blade (Figure 7), which reveal that the effective light yield of GLO(Eu) is ~7.5x higher than the IQI Tb-glass, and the spatial resolution is also slightly improved by a factor of ~1.2. Computed tomography reconstructions of the nickel turbine blade, shown in Figure 8, reveal that the higher light yield and good resolution of the GLO(Eu) scintillator provides a crisper, higher contrast image.

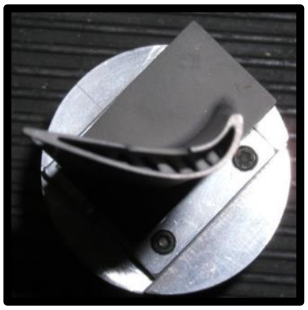

Scintillator	Attenuation Radiograph (2 frame average, 12s)	CT reconstruction (5 slice average), 540 view, 360° half scan	LY (cts/s)	Resolution (lp/mm)
Tb-glass 	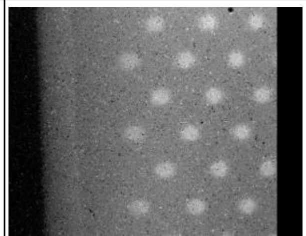	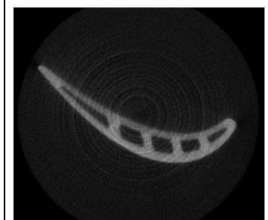	63	7.3
GLO 	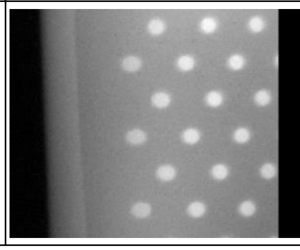	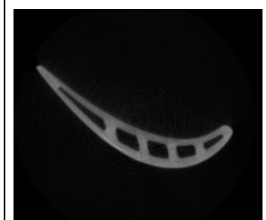	475	8.5
Improvement:			7.5X	1.2X

Figure 7. Photograph of a single crystal nickel turbine blade, used for 9 MeV computed tomography studies.

Figure 8. **(left)** Photos of IQI Tb-glass and GLO transparent ceramic scintillators. Images acquired of the turbine blade, with internal structural pillars. **(middle)** Attenuation radiographs showing the internal pillars. **(right)** Computed tomography reconstructions indicate improved contrast, resolution, and reduction in ring artifacts for the images acquired with the GLO(Eu) transparent ceramic scintillator.

4. CONCLUSIONS

Transparent ceramic GYGAG(Ce) offers high light yield and gamma spectroscopy with better resolution than NaI(Tl). It can be instrumented with PMT or Silicon photodiode readout, providing energy resolution R(662 keV) < 5%. With photodiode readout resolution as good as R(662 keV) = 3% can be obtained. Transparent ceramic GLO(Eu) can improve throughput for MeV radiography. It has been scaled up to 10” diameter optically transparent sheets that offer spatial resolution slightly better than the standard glass scintillator, while the combined light yield and stopping power improvement results in >7x higher effective light yield.

ACKNOWLEDGEMENTS

This work was performed under the auspices of the U.S. DOE by Lawrence Livermore National Laboratory under Contract DE-AC52-07NA27344. We are grateful to the US Department of Homeland Security, Domestic Nuclear Detection Office, for funding the development of the garnet transparent ceramics under competitively awarded IAA HSHQDC-12-X-00149. We are grateful to William McLean, Beverly Hobson and George Overturf for funding the development of the bixbyite scintillator for the US DOE National Nuclear Security Administration, Enhanced Surveillance Campaign. This support does not constitute an express or implied endorsement on the part of the Government.

REFERENCES

[1] S.F. Wang, J. Zhang, D.W. Luo, F. Gu, D.Y. Tang, Z.L. Dong, G.E.B. Tan, W.X. Que, T.S. Zhang, S. Li, L.B. Kong, “Transparent ceramics: Processing, materials and applications,” Prog. Sol. St. Chem., 41, 20-54 (2013).

[2] L.B. Kong, Y. Huang, W. Que, T. Zhang, S. Li, J. Zhang, Z. Dong, D. Tang, Transparent Ceramics, Springer International Publishing Switzerland (2015).

[3] J. Li, Y. Pan, Y. Zeng, W. Liu, B. Jiang, J. Guo., “The history, development, and future prospects for laser ceramics: A review,” Internat. J. Refractory Met. Hard Mat., 39, 44-52 (2013).

[4] M. Rubat du Merac, H.-J. Kleebe, M.M. Müller and I.E. Reimanis, “Fifty Years of Research and Development Coming to Fruition; Unraveling the Complex Interactions during Processing of Transparent Magnesium Aluminate (MgAl2O4) Spinel.” J. Am. Ceram. Soc., 96 [11] 3341–3365 (2013).

[5] J.W. McCauley, P. Patel, M.Chen, G. Gilde, E. Strassburger, B. Paliwal , K.T. Ramesh, D.P. Dandekar “AlON: A brief history of its emergence and evolution,” J. European Ceram. Soc., 29, 223–236, (2009).

[6] G. Hull, J.J. Roberts, J.D. Kuntz, S.E. Fisher, R.D. Sanner, T.M. Tillotson, A.D. Drobshoff, S.A. Payne, and N.J. Cherepy, “Ce-doped single crystal and ceramic Garnets for□□□ ray detection” Proc. SPIE 6706, 670617 (2007).

[7] N.J. Cherepy, J.D. Kuntz, J.J. Roberts, T.A. Hurst, O.B. Drury, R.D. Sanner, T.M. Tillotson, S.A. Payne, “Transparent Ceramic Scintillator Fabrication, Properties and Applications,” Proc. SPIE, 7090, 707917 (2008).

[8] Cherepy, N.J.; Kuntz, J.D.; Seeley, Z.M.; Fisher, S.E.; Drury, O.B.; Sturm, B.W.; Hurst, T.A.; Sanner, R.D.; Roberts, J.J.; Payne, S.A., “Transparent ceramic scintillators for γ spectroscopy and radiography,” Proc. SPIE, 7805, 7805-01 (2010).

[9] N.J. Cherepy, S.A. Payne, B.W. Sturm, J.D. Kuntz, Z.M. Seeley, B.L. Rupert, R.D. Sanner, O.B. Drury, T.A. Hurst, S.E. Fisher, M. Groza, L. Matei, A. Burger, R. Hawrami, K.S. Shah, L.A. Boatner, “Comparative gamma spectroscopy with SrI2(Eu), GYGAG(Ce) and Bi-loaded plastic scintillators,” IEEE Nuc. Sci. Symp. Conf. Record, p. 1288 - 1291 (2010).

[10] N.J. Cherepy, S.A. Payne, B.W. Sturm, S.P O’Neal, Z.M. Seeley, O.B. Drury, L.K. Haselhorst, B.L. Rupert, R.D. Sanner, P.A. Thelin, S.E. Fisher, R. Hawrami, K.S. Shah, A. Burger, J. O. Ramey, L.A. Boatner, “Performance of Europium-Doped Strontium Iodide, Transparent Ceramics and Bismuth-loaded Polymer Scintillators,” Proc. SPIE, 8142, 81420W (2011).

[11] Z.M. Seeley, N.J. Cherepy, S.A. Payne, “Homogeneity of Gd-based garnet transparent ceramic scintillators for gamma spectroscopy,” Journal of Crystal Growth 379, 79-83 (2013).

[12] N.J. Cherepy, Z.M. Seeley, S.A. Payne, P.R. Beck, O.B. Drury, S.P. O’Neal, K. Morales Figueroa, S. Hunter, L. Ahle, P.A. Thelin, T. Stefanik, J. Kindem, “Development of Transparent Ceramic Ce-Doped Gadolinium Garnet Gamma Spectrometers,” IEEE Trans. Nucl. Sci., 60,3, 2330 (2013).

[13] Z.M. Seeley, N.J. Cherepy, S.A. Payne, “Expanded Phase Stability of Gd-Based Garnet Transparent Ceramic Scintillators,” Journal of Materials Research 29, 2332-2337 (2014).

[14] Z. Seeley, N. Cherepy, S. Payne, “Two-step sintering of Gd0.3Lu1.6Eu0.1O3 transparent ceramic scintillator,” Optical Materials Express 3, 908-912 (2013).

[15] J.E. Trebes, K.W. Dolan, W.S. Haddad, J.J. Haskins, R.A. Lerche, C.M. Logan, D.E. Perkins, D.J. Schneberk, R.D. Rikard, “High Resolution, Large Area, High Energy X-Ray Tomography,” Proc. SPIE. 3149, Developments in X-Ray Tomography, 173, 0277-786X (1997).

[16] A. Lempicki, et al, Nuc. Inst. Meth. Phys. Res. A, 488 (2002) 579.

[17] V. Nagarkar, et al, Nuc. Inst. Meth. Phys. Res. B, 213 (2004) 250.

[18] Z. M. Seeley, Z. R. Dai, J. D. Kuntz, N. J. Cherepy, S. A. Payne, Opt. Mater. 35, 74 (2012).

[19] L. Mädler, H.K. Kammler, R. Mueller, S.E. Pratsinis, “Controlled synthesis of nanostructured particles by flame spray pyrolysis,” Aerosol Sci. 33, 369 (2002).

[20] C.R. Bickmore, K.F. Waldner, D.R. Treadwell, R.M. Laine, "Ultrafine Spinel Powders by Flame Spray Pyrolysis of a Magnesium Aluminum Double Alkoxide," J. Am. Ceram. Soc., 79, 1419-23 (1996).

[21] J. Kindem, R. Conwell, Z.M. Seeley, N.J. Cherepy, S.A. Payne, “Performance Comparison of Small GYGAG(Ce) and CsI(TI) Scintillators with PIN Detectors,” IEEE Nuclear Science Symposium, Conf. Record, (2011).

[22] R. Brancaccio, M. Bettuzzi, F. Casali, M.P. Morigi, G. Levi, A. Gallo, G. Marchetti, D. Schneberk., IEEE Trans. Nucl. Sci., 58, 4, 1864-1871 (2011).

[23] NJ Cherepy, ZM Seeley, SA Payne, PR Beck, EL Swanberg, S Hunter, L Ahle, SE Fisher, C Melcher, H Wei, T Stefanik, Y-S Chung, J Kindem, High energy resolution with transparent ceramic garnet scintillators Proc. SPIE, 921302-921302-6 (2104).

[24] E. Swanberg, et al. IEEE Trans. Nucl. Sci., submitted (2015).